


# A Retrospectively Study: Diagnosis of Pathological Types of Malignant Lung Tumors by Dual-layer Detector Spectral Computed Tomography

Technology in Cancer Research & Treatment  
Volume 21: 1-9  
© The Author(s) 2022  
Article reuse guidelines:  
sagepub.com/journals-permissions  
DOI: 10.1177/15330338221074498  
journals.sagepub.com/home/tct  


Xia Ma, MD<sup>1</sup> , Ming Xu, BD<sup>2</sup>, Xiao-Juan Tian, MD<sup>2</sup>, Yong-Li Liu, BD<sup>2</sup>, Xin-Ri Zhang, PhD<sup>2</sup>, and Ying Qiao, PhD<sup>2</sup>

## Abstract

**Object:** By retrospectively analyzing the energy spectrum of squamous cell carcinoma, adenocarcinoma, small cell lung cancer (SCLC), and pulmonary metastases that underwent dual-layer detector spectral computed tomography (DLCT) 3-phase scan of the chest, we explored the value of a multiparameter energy spectrum in the assessment of pathological types of lung tumors. **Methods:** Cases of squamous cell carcinoma ( $n=20$ ), adenocarcinoma ( $n=24$ ), SCLC ( $n=26$ ), and metastases ( $n=14$ ) were collected. Then the largest cross-sectional area (LCA) of the lesion, computed tomography (CT) values in the plain scan phase, arterial and venous phases (HU, HUa, and HUv), iodine concentration, and effective atomic number in the arterial and venous phases (ICa, ICv, Zeff[a], and Zeff[v]) were measured and compared among the nonsmall cell lung cancer (NSCLC), SCLC and metastases, and other 3 groups of SCLC, squamous cell carcinoma, and adenocarcinoma. **Results:** Only the LCA is statistically different among SCLC, NSCLC, and metastases ( $P < .05$ ). And the treated subgroup analysis did not show significant differences among the groups. However, the untreated subgroup analysis showed that there was a significant difference between NSCLC and metastases in LCA, SCLC and metastases in ICa, NSCLC and SCLC in HUv, NSCLC and SCLC in Zeff(v) ( $P < .05$ ). **Conclusion:** The energy spectrum parameters of DLCT have a certain clinical value in distinguishing NSCLC from SCLC in the Zeff(v) and distinguishing SCLC from metastases in the ICa.

## Keywords

lung tumor, spectral CT, effective atomic number, x-ray, computed tomography

## Abbreviations

CT, computed tomography; DECT, dual-energy CT; DLCT, detector spectral CT; LCA, largest cross-sectional area; NSCLC, nonsmall cell lung cancer; SCLC, small cell lung cancer.

Received: October 19, 2021; Revised: November 14, 2021; Accepted: January 2, 2022.

## Introduction

Lung cancer is a common malignant tumor worldwide. In 2008, lung cancer replaced liver cancer as the leading cause of death in China's malignant tumor population. According to statistics, 600,000 people die of lung cancer in China every year.<sup>1</sup> The lung is a common metastatic site for malignant tumors throughout the body. Clarifying the histopathological type of tumor is the basis for judging its biological behavior, formulating a reasonable treatment plan, and prognostic evaluation.

<sup>1</sup> Beijing Youan Hospital, Capital Medical University, Beijing, China

<sup>2</sup> The First Hospital of Shanxi Medical University, Taiyuan, China

### Corresponding Authors:

Xin-Ri Zhang, Department of Pulmonary and Critical Care Medicine, The First Hospital Of Shanxi Medical University, Taiyuan, China.  
Email: ykdzxr61@163.com

Ying Qiao, Imaging Department, The First Hospital Of Shanxi Medical University, Taiyuan, China.  
Email: 15103462912@163.com



Therefore, accurately judging the type is the key to tumor staging and optimizing treatment. Although the histopathological examination is the gold standard for lung cancer classification, it must be obtained through invasive methods such as surgical resection or needle biopsy, which may not only cause many complications, but sometimes it is impossible to accurately determine the type.<sup>2</sup> Therefore, how to use noninvasive methods to determine the type of diseased tissue is always the goal of exploration.

Dual-energy computed tomography (CT), which has imaging characteristics such as multiparameter and quantitative analysis, is a new technology in the CT imaging field in recent years. It can objectively reflect the tissue characteristics of the lesion through the comprehensive application of multiple parameters and analysis tools. Therefore, it has a potential value in determining the tissue source and scope of the disease, differential diagnosis, and efficacy evaluation. It has also achieved preliminary results in research on lung cancer screening and the determination of benign and malignant lung nodules.<sup>3</sup> Dual-layer detector spectral CT (DLCT) is the latest generation of dual-energy CT technology and its images can be reconstructed on the basis of original data. Compared with other dual-energy CT based on tubes, DLCT has certain technical advantages, and its application is worthy of further exploration in clinical research.<sup>4</sup>

## Methods

### Research Object

This retrospective, single-center study was approved by our institutional review board, and a waiver of informed consent was obtained. Before the examination, an enhanced CT consent form was routinely signed, and all patient details were de-identified during the research. A total of 84 cases (60 males and 24 females), including 72 patients who underwent DLCT scans in our hospital from June to December 2019 and were pathologically diagnosed with lung tumors, and 12 cases clinically diagnosed with metastatic tumors by CT were consecutively collected. Among these cases, there were 20 squamous cell carcinomas, 24 adenocarcinomas, 26 small cell lung cancer (SCLC), and 14 metastatic tumors. The primary sites of 14 cases of metastatic tumors were hepatocellular carcinoma, mesenteric leiomyosarcoma, bladder cancer, adrenal cortex cancer, cardia adenocarcinoma, breast cancer, laryngeal cancer, colon cancer, rectal cancer, urothelial cancer, kidney cancer, breast cancer, rectal cancer, and thymoma, respectively. Among the 84 cases, 51 cases did not receive treatment before the examination. Pathological findings included 33 cases of fiber optic bronchoscopy biopsy, 26 cases of lung biopsy, 5 cases of cervical lymph node puncture, 4 cases of surgical resection, 1 case of pleural effusion cytology, 1 case of pericardial effusion cytology, 1 case of mediastinal lymph node puncture, and 1 case of thoracoscopic biopsy. Twelve cases of metastatic tumors were clinically diagnosed by CT. Among the 84 patients, 56 patients were treated, including squamous cell carcinomas ( $n$

= 13), adenocarcinomas ( $n = 14$ ), SCLC ( $n = 20$ ), and metastatic tumors ( $n = 9$ ).

### Scanning Methods

All patients underwent a chest plain scan and enhanced scan by using the conventional mode of DLCT (iQon, Phillips). Contrast agent (Iomeprol, Imeron 400 MCT, 400 mg/mL; Bracco Imaging Deutschland GmbH) was administered intravenously at a dose of 1.2 ml/kg at a flow rate of 2 to 2.5 mL/s, and then injected 30 mL normal saline at the same flow rate. The scan delay time after the contrast agent injection is 35 s and 65 s, which are considered to be the arterial and venous phase scans respectively. Scanning parameters: 120 kVp; automatic tube current (37–84 mAs); matrix 512 × 512; collimation 64 × 0.625 mm; reconstruction thickness and interval 0.9 mm/0.9 mm. Regular and spectral images were reconstructed using iDose4 and spectral level 6 (Philips Healthcare) reconstruction algorithms. The average volume-weighted CT dose index and dose length product are 4.4 mGy and 180 mGy\*cm, respectively, corresponding to an effective dose of 2.5 mSv (conversion coefficient: 0.014). The scanning range is from the apex of the lungs to the level of the septal muscles, and the patient is asked to complete it under breath-holding. All patients had signed an informed consent form before undergoing enhanced scanning.

### Image Postprocessing and Quantitative Measurement

A hospitalized radiologist with 3 years of radiology experience and a senior radiologist with 11 years of radiology experience jointly performed quantitative measurements of spectral data on an ISP workstation (IntelliSpace Portal v. 10.1, Philips Healthcare). In each patient, the lesion volume was semiautomatically segmented on the axial plane of the plain scan image, and the soft tissue window was set to produce the lung lesions of interest. Based on spectral image reconstruction, the software provides traditional CT images, effective atomic number images, and iodine density maps at the same time. For each patient, the following parameters of the solid part of the lesion of interest were obtained and recorded: the LCA of the lesion ( $\text{mm}^2$ ), the CT value (HU, HUa, HUv) of the plain, arterial and venous phases, iodine concentration (mg/ml) (ICa, ICv) and effective atomic number ( $Z_{\text{eff}}[a]$ ,  $Z_{\text{eff}}[v]$ ) of the arterial and venous phases.

### Statistical Analysis

SPSS22.0 software was used to analyze the measured data. All continuous variables were tested for normality and were represented by the mean  $\pm$  standard deviation or median (interquartile range). Categorical variables were represented by numbers (%). Chi-square test, one-way variance analysis, or Kruskal–Wallis H test was applied to compare and analyze multiple groups. Bonferroni method was used in pairwise comparison. Differences between means were assessed by pairwise

**Table 1.** Comparison of Clinical Characteristics and CT Indexes of NSCLC, SCLC, and Metastatic Tumors.

	NSCLC (n = 44)	SCLC (n = 26)	Metastatic tumors (n = 14)	P-value
Age (year)	63.18 ± 9.55	61.04 ± 8.36	60.43 ± 10.11	.503
Gender				.146
Male	30 (68.2%)	20 (76.9%)	8 (57.1%)	
Female	14 (31.8%)	4 (23.1%)	6 (42.9%)	
Smoking history				.092
Yes	21 (47.7%)	7 (37.1%)	3 (17.6%)	
No	23 (42.3%)	19 (62.9%)	14 (82.4%)	
Weight	61.70 ± 11.86	66.00 ± 11.33	61.21 ± 10.91	.272
LCA (mm <sup>2</sup> )	572.85 (1823.76)	302.64 (647.44)	83.26 (158.31**)	.001
HU	40.79 (13.40)	42.13 ± 9.24	33.25 (28.70)	.204
HUa	64.27 ± 11.47	59.43 ± 11.68	61.37 ± 23.80	.190
HUv	67.70 ± 11.68	60.95 (24.68)	61.69 ± 18.06	.242
ICa (mg/ml)	1.24 ± 0.42	0.97 (0.62)	1.50 ± 1.01	.381
ICv (mg/ml)	1.30 ± 0.43	1.10 (0.53)	1.43 ± 0.82	.539
Zeff(a)	7.97 (0.28)	7.85 (0.26)	8.07 ± 0.57	.232
Zeff(v)	7.98 ± 0.22	7.90 (0.31)	8.05 ± 0.44	.129

Abbreviations: CT, computed tomography; NSCLC, nonsmall cell lung cancer; SCLC, small cell lung cancer; LCA, largest cross-sectional area.

\*Compared with NSCLC,  $P < .05$ . #Compared with SCLC,  $P < .05$ .

Welch's  $t$ -test to correct for unequal variances between groups. Multiple testings were computed using the Games–Howell test.  $P < .05$  indicates that the difference is statistically significant.

between nonsmall cell lung cancer (NSCLC) and metastases, and between SCLC and metastases were discovered statistical differences, respectively ( $P < .05$ ) (Table 1).

## Results

### Comparison of Nonsmall Cell Lung Cancer, SCLC, and Metastases

There was no statistical difference in clinical characteristics of 84 patients, 20 squamous cell carcinomas, 24 adenocarcinomas, 26 SCLC, and 14 metastatic tumors (Table 1). A total of 8 CT indicators were included in the study, however, only the LCA

### Comparison of Squamous Cell Carcinoma, Adenocarcinoma, and SCLC

In 70 patients, the clinical characteristics of adenocarcinoma ( $n = 24$ ), squamous cell carcinoma ( $n = 20$ ), and SCLC ( $n = 26$ ) were statistically different in gender ( $P = .003$ ). And there is a statistically significant difference between the squamous cell carcinoma and the adenocarcinoma group in gender ( $P = .008$ ) (Table 2). Among the 8 CT indicators, only LCA was statistically

**Table 2.** Comparison of Clinical Characteristics and CT Indexes of Squamous Cell Carcinoma, Adenocarcinoma, and SCLC.

	Squamous cell carcinoma (n = 20)	Adenocarcinoma (n = 24)	SCLC (n = 26)	P-value
Age (year)	65.25 ± 6.91	61.04 ± 8.36	61.46 ± 11.14	0.251
Gender				0.003
Male	18 (90.0%)	12 (50.0%) *	22 (84.6%)	
Female	14 (10.0%)	12 (50.0%) *	4 (15.4%)	
Smoking history				0.072
Yes	12 (60.0%)	9 (37.5%)	7 (29.6%)	
No	8 (40.0%)	15 (62.5%)	19 (73.1%)	
Weight	59.05 ± 7.96	63.91 ± 14.12	61.21 ± 10.91	0.382
LCA (mm <sup>2</sup> )	1255.60 (2738.66)	306.08 (1357.55)	302.64 (647.44)#	0.011
HU	42.30 (12.9)	40.40 (13.48)	42.13 ± 9.24	0.854
HUa	61.94 ± 11.98	66.11 ± 10.96	59.43 ± 11.68	0.122
HUv	65.17 ± 13.85	69.69 ± 9.46	60.95 (24.7)	0.170
ICa (mg/ml)	1.14 ± 0.44	1.33 ± 0.39	0.97 (0.64)	0.124
ICv (mg/ml)	1.26 ± 0.51	1.34 ± 0.36	1.10 (0.53)	0.445
Zeff(a)	7.94 (0.55)	8.00 (0.27)	7.85 (0.25)	0.106
Zeff(v)	7.96 ± 0.29	8.00 ± 0.13	7.90 (0.30)	0.099

Abbreviations: CT, computed tomography; SCLC, small cell lung cancer; LCA, largest cross-sectional area.

\*Compared with squamous cell carcinoma,  $P = .008$ . #Compared with squamous cell carcinoma,  $P = .012$ .

**Table 3.** Comparison of Clinical Characteristics and CT Indexes of Untreated NSCLC, SCLC, and Metastases.

	NSCLC (n = 30)	SCLC (n = 12)	Metastases (n = 9)	P-value
Age (year)	62.77 ± 9.00	60.75 ± 9.36	60.78 ± 12.32	.770
Gender				
Male	21 (70.0%)	10 (83.3%)	5 (55.6%)	.366
Female	9 (30.0%)	2 (16.7%)	4 (44.4%)	
Smoking history				
Yes	15 (50%)	3 (25.0%)	1 (11.1%)	.077
No	15 (50%)	9 (75.0%)	8 (88.9%)	
Weight	60.98 ± 10.75	63.17 ± 9.36	59.89 ± 8.85	.738
LCA (mm <sup>2</sup> )	1017.12 (2938.18)	291.20 (717.78)	104.44 (101.57) *	.001
HU	43.91 ± 11.42	40.36 ± 8.25	33.70 (31.90)	.288
Hua	64.28 ± 10.34	57.21 ± 13.20	62.46 ± 28.81	.240
HUv	68.38 ± 10.87	58.19 ± 14.66*	58.78 ± 20.94	.031
ICa (mg/ml)	1.24 ± 0.42	0.92 (0.56)	1.90 ± 0.94#	.024
ICv (mg/ml)	1.32 ± 0.37	1.11 ± 0.31	1.60 ± 0.87	.144
Zeff(a)	7.95 (0.27)	7.84 ± 0.30	8.25 ± 0.59	.187
Zeff(v)	8.00 ± 0.17	7.78 ± 0.23*	8.11 ± 0.49	.014

Abbreviations: CT, computed tomography; NSCLC, nonsmall cell lung cancer; SCLC, small cell lung cancer; LCA, largest cross-sectional area.

\*Compared with NSCLC,  $P < .05$ . #Compared with SCLC,  $P < .05$ .

different among the 3 groups ( $P = .011$ ), and between the squamous cell carcinoma group and the SCLC group ( $P = .012$ ) (Table 2).

and SCLC ( $P = .045$ ,  $.016$ ). Between NSCLC and metastases groups, only LCA was statistically different ( $P < .001$ ). And there was a significant difference in ICa between SCLC and metastases ( $P = .021$ ) (Table 3).

### Comparison of Untreated NSCLC, SCLC, and Metastases

In the untreated 51 patients, there was no statistical difference in clinical characteristics among NSCLC ( $n = 30$ ), SCLC ( $n = 12$ ), and metastatic tumor ( $n = 9$ ) groups. Among the 8 CT indexes, the LCA, the HUv, the ICa, and the Zeff(v) were statistically different among the 3 groups ( $P < .05$ ). HUv and Zeff(v) were statistically different between NSCLC

### Comparison of Untreated Squamous Cell Carcinoma, Adenocarcinoma, and SCLC

Among the 42 untreated patients, the gender of squamous cell carcinoma ( $n = 14$ ), adenocarcinoma ( $n = 16$ ), and SCLC ( $n = 12$ ) were statistically different ( $P = .019$ ). Among them, there were significant differences between the adenocarcinoma and squamous cell carcinoma group ( $P = .017$ ). Among the 8 CT indicators, the

**Table 4.** Comparison of Clinical Characteristics and CT Indexes of Untreated Squamous Cell Carcinoma, Adenocarcinoma, and SCLC.

	Squamous cell carcinoma (n = 14)	Adenocarcinoma (n = 16)	SCLC (n = 12)	P-value
Age (year)	63.43 ± 6.38	62.19 ± 10.97	60.75 ± 9.36	.553
Gender				.019
Male	13 (92.9%)	8 (50.0%) *	10 (83.3%)	
Female	1 (7.1%)	8 (50.0%) *	2 (16.7%)	
Smoking history				.038
Yes	10 (71.4%)	5 (31.3%)	3 (25.0%)	
No	4 (28.6%)	11 (68.7%)	9 (75.0%)	
Weight	58.81 ± 7.43	63.17 ± 9.36	62.88 ± 12.93	.473
LCA (mm <sup>2</sup> )	2350.33 ± 1786.78	306.07 (1042.35)	291.20 (717.78) #	.013
HU	41.63 ± 12.9	45.76 ± 13.07	40.36 ± 8.25	.370
HUa	62.56 ± 11.29	65.68 ± 9.64	57.21 ± 13.20	.152
HUv	68.31 ± 11.89	68.44 ± 10.37	58.19 ± 14.66	.056
ICa (mg/ml)	1.17 ± 0.42	1.31 ± 0.42	0.92 (0.56)	.542
ICv (mg/ml)	1.32 ± 0.41	1.33 ± 0.35	1.11 ± 0.31	.255
Zeff(a)	7.89 (0.34)	7.97 ± 2.23	7.84 ± 0.30	.228
Zeff(v)	8.00 ± 0.21	8.01 ± 0.14	7.78 ± 0.23#^	.005

Abbreviations: CT, computed tomography; SCLC, small cell lung cancer; LCA, largest cross-sectional area.

\*Compared with squamous cell carcinoma,  $P = .017$ . #Compared with squamous cell carcinoma,  $P < .05$ . ^Compared with adenocarcinoma,  $P < .05$ .

**Table 5.** Comparison of CT Indexes of NSCLC, SCLC, and Metastatic Tumor (LCA < 300 mm<sup>2</sup>).

	NSCLC (n = 11)	SCLC (n = 7)	Metastatic tumors (n = 9)	P-value
LCA (mm <sup>2</sup> )	198.54 ± 73.93	148.88 ± 110.45	104.44 (101.57)	.133
HU	47.93 ± 14.61	42.59 ± 7.78	33.70 (31.90)	.246
HUa	65.96 ± 9.50	51.29 ± 6.89*	62.46 ± 28.81	.008
HUv	68.28 ± 12.57	55.29 ± 12.33	58.79 ± 20.94	.207
ICa (mg/ml)	1.29 ± 0.48	0.85 (0.47)	1.90 ± 0.94	.057
ICv (mg/ml)	1.35 ± 0.42	1.14 ± 0.37	1.60 ± 0.87	.332
Zeff(a)	7.92 ± 0.25	7.80 ± 0.33	8.25 ± 0.59	.089
Zeff(v)	7.99 ± 0.17	7.81 ± 0.24	8.11 ± 0.49	.285

Abbreviations: CT, computed tomography; NSCLC, nonsmall cell lung cancer; SCLC, small cell lung cancer; LCA, largest cross-sectional area.

\*Compared with NSCLC, P = .004.

LCA and the Zeff(v) were statistically different among the 3 groups (P < .05). Between the SCLC and the squamous cell carcinoma groups, significant differences were discovered in LCA and Zeff(v) (P = .022, .015). And between SCLC and adenocarcinoma groups, only Zeff is statistically different (P = .008) (Table 4).

**Comparison of Untreated NSCLC, SCLC, and Metastases with Similar LCA**

Among the 27 untreated patients of NSCLC (n = 11), SCLC (n = 7), and metastases (n = 9) (LCA < 300 mm<sup>2</sup>), HUa was statistically different among the 3 groups (P = .008). In multiple comparisons, statistical differences were discovered between NSCLC and SCLC (P = .004) (Table 5).

**Comparison of Untreated Squamous Cell Carcinoma, Adenocarcinoma, and SCLC with Similar LCA**

Among the 27 untreated patients of squamous cell carcinoma (n = 5), adenocarcinoma (n = 12), and SCLC (n = 10) (LCA < 1000 mm<sup>2</sup>), the HUa and the Zeff(v) were statistically different among the 3 groups (P < .05). In addition, a significant difference was discovered in the Zeff(v) between SCLC and adenocarcinoma groups (P = .029). But in the post hoc tests of HUa, no significant difference was discovered between SCLC and adenocarcinoma group (P = .065) (Table 6).

**Comparison of NSCLC, SCLC, and Metastases After Treatment**

In the 56 patients after treatment (including the posttreatment data of 23 patients in the untreated group), there was no statistical difference in clinical characteristics and CT indexes among NSCLC (n = 27), SCLC (n = 20), and metastatic tumor (n = 9) groups (Table 7).

**Comparison of Squamous Cell Carcinoma, Adenocarcinoma, and SCLC with Similar LCA After Treatment**

In 47 patients, the clinical characteristics and CT indexes showed no statistical differences among squamous cell carcinoma (n = 13), adenocarcinoma (n = 14), and SCLC (n = 20) (P > .05) (Table 8).

**Discussion**

According to the histological type, lung cancer is divided into 2 main subtypes: NSCLC and SCLC, and then the most common types of NSCLC are squamous cell carcinoma and adenocarcinoma. Lung metastases are also very common and sometimes difficult to distinguish from the primary lung tumor. As the preferred imaging method for chest diseases, CT has an important value in the diagnosis of lung tumors. Ordinary CT diagnosis

**Table 6.** Comparison of CT Indexes of Untreated Squamous Cell Carcinoma, Adenocarcinoma, and SCLC (LCA < 1000 mm<sup>2</sup>).

	Squamous cell carcinoma (n = 5)	Adenocarcinoma (n = 12)	SCLC (n = 10)	P-value
LCA (mm <sup>2</sup> )	410.95 ± 142.20	187.41 (268.87)	292.65 ± 273.98	.278
HU	34.70 ± 8.86	45.84 ± 15.14	39.59 ± 8.24	.470
HUa	53.18 ± 8.46	65.64 ± 10.98	54.31 ± 11.40	.033
HUv	57.50 ± 9.49	67.74 ± 11.81	58.51 ± 16.10	.197
ICa (mg/ml)	1.15 ± 0.65	1.30 ± 0.47	0.92 (0.47)	.302
ICv (mg/ml)	1.33 ± 0.51	1.36 ± 0.40	1.13 ± 0.33	.348
Zeff(a)	7.93 ± 0.38	7.94 ± 0.25	7.84 ± 0.28	.691
Zeff(v)	7.84 ± 0.20	8.01 ± 0.16	7.79 ± 0.20#	.025

Abbreviations: CT, computed tomography; SCLC, small cell lung cancer; LCA, largest cross-sectional area.

#Compared with adenocarcinoma, P < .05.

**Table 7.** Comparison of Clinical Characteristics and CT Indexes of NSCLC, SCLC, and Metastases After Treatment.

	NSCLC (n = 27)	SCLC (n = 20)	Metastatic tumors (n = 9)	P-value
Age (year)	63.11 ± 9.80	60.89 ± 7.59	61.11 ± 4.88	.567
Gender				.146
Male	20 (74.1%)	16 (80%)	4 (44.4%)	
Female	7 (25.9%)	4 (20%)	5 (55.6%)	
Smoking history				.262
Yes	13 (48.1%)	6 (30%)	2 (22.2%)	
No	14 (51.9%)	14 (70%)	7 (77.8%)	
Weight	66.22 ± 13.03	60.00 (14.00)	56.06 ± 7.95	.086
LCA (mm <sup>2</sup> )	252.15 (1967.55)	300.99 (617.82)	109.31 ± 95.86	.112
HU	40.24 ± 11.00	41.59 ± 6.98	42.07 ± 7.55	.847
HUa	60.10 (18.40)	63.56 ± 14.29	66.52 ± 12.20	.420
HUv	66.60 ± 12.93	65.53 ± 13.65	62.63 ± 14.27	.727
ICa (mg/ml)	0.94 (0.55)	1.36 ± 0.77	1.27 ± 0.50	.374
ICv (mg/ml)	1.12 (0.48)	1.53 ± 0.79	1.23 ± 0.51	.299
Zeff(a)	7.83 (0.43)	7.92 (0.57)	7.97 ± 0.33	.454
Zeff(v)	7.94 (0.21)	7.95 (0.60)	7.90 ± 0.33	.552

Abbreviations: CT, computed tomography; NSCLC, nonsmall cell lung cancer; SCLC, small cell lung cancer; LCA, largest cross-sectional area.

of lung tumors mainly focuses on morphology, and the pathological classification is mainly based on clinical experience to make preliminary inferences.

A well-known shortcoming of ordinary CT is that different substances and tissues may show similar attenuation levels at a single radiation energy level, that is, different tissues have similar CT values. Dual-energy CT (DECT), which uses material decomposition, is a noninvasive functional imaging method that can quantitatively measure tissue perfusion parameters and energy spectrum parameters and can noninvasively and quantitatively reflect changes in the metabolism and blood flow of the lesion. It has important clinical value in many aspects.<sup>3,5,6</sup>

DLCT has several advantages compared with other DECT. Firstly, because the original data obtained by DLCT can be used to retrospectively reconstruct traditional CT images at

the projection level, there is no need to choose between traditional and spectral imaging before scanning. Hokamp et al<sup>7</sup> showed that the attenuation characteristics of the 72 keV single-energy image are almost the same as the traditional image, while the image quality has been improved. Secondly, the high- and low-energy level imaging is obtained in the same space and angle at the same time, so the imaging of moving organs is more ideal. Thirdly, because DLCT can be reconstructed on the basis of the original data, other DECT mostly reconstruct at the image level, for example, spectral imaging can be reconstructed at the projection level, but time and angle interpolation are required before reconstruction, its low-energy class-level virtual single-energy image quality is better, which is more conducive to the selection of measurement positions.<sup>8</sup>

**Table 8.** Comparison of Clinical Characteristics and CT Indexes of Squamous Cell Carcinoma, Adenocarcinoma, and SCLC After Treatment.

	Squamous cell carcinoma (n = 13)	Adenocarcinoma (n = 14)	SCLC (n = 20)	P-value
Age (year)	66.38 ± 6.91	60.07 ± 11.11	60.89 ± 7.59	.113
Gender				.087
Male	12 (92.3%)	8 (57.1%)	16 (80.0%)	
Female	1 (7.7%)	6 (42.9%)	4 (20.0%)	
Smoking history				.446
Yes	6 (46.2%)	7 (50.0%)	6 (30.0%)	
No	7 (53.8%)	7 (50.0%)	14 (70.0%)	
Weight	69.31 ± 7.21	63.36 ± 12.94	60.00 (14.00)	.218
LCA (mm <sup>2</sup> )	527.46 (2587.62)	878.29 (1698.99)	300.99 (617.82)	.715
HU	38.41 ± 6.59	41.94 ± 12.16	41.59 ± 6.98	.555
HUa	58.00 (21.45)	60.66 ± 10.47	63.56 ± 14.29	.729
HUv	64.84 ± 13.66	68.22 ± 12.50	65.53 ± 13.65	.621
ICa (mg/ml)	1.00 (0.76)	0.96 ± 0.77	1.36 ± 0.77	.429
ICv (mg/ml)	1.07 (0.53)	1.23 ± 0.33	1.53 ± 0.79	.195
Zeff(a)	7.90 (0.53)	7.83 ± 0.31	7.92 (0.57)	.742
Zeff(v)	7.87 (1.58)	7.98 ± 0.15	7.95 (0.60)	.307

Abbreviations: CT, computed tomography; SCLC, small cell lung cancer; LCA, largest cross-sectional area.

In this study, after analyzing all cases that have undergone radiotherapy, chemotherapy, or targeted therapy, no statistically different indicators were found except for LCA. The untreated subgroup analysis showed that compared with NSCLC, the HUv and the Zeff(v) of SCLC were significantly low ( $P < .05$ ), and the untreated subgroup analysis of similar LCAs showed that HUA of SCLC is significantly lower than NSCLC's ( $P < .05$ ), which may be related to the lower capillary permeability of SCLC. Spira et al<sup>9</sup> used volume perfusion CT and histopathological results to assess the vascular correlation of lung cancer, and confirmed that compared with adenocarcinoma, the transmission constant of the parameter representing capillary permeability in SCLC was reduced.

In this study, although no statistical difference was observed, compared with NSCLC, the arterial phase CT value, arteriovenous phase iodine concentration, and arterial phase effective atomic number of SCLC were lower. These differences can be explained by the obvious differences in blood vessels and vasculature between SCLC and NSCLC. Compared with SCLC, the vascular beds of adenocarcinoma and squamous cell carcinoma are composed of many large blood vessels, which allow larger tumor blood volume and higher CT values

in the arteriovenous phase.<sup>10,11</sup> In addition, compared with NSCLC, tumor necrosis in SCLC is more common and widespread. Shi et al<sup>12</sup> also discovered that compared with SCLC, the dynamic volume perfusion CT parameters, including blood volume, blood flow, and permeability adenocarcinoma and squamous cell carcinoma were significantly higher.

Moreover, the untreated subgroup analysis showed that the arterial iodine concentration of metastases was significantly higher than that of SCLC ( $P < .05$ ). Although no statistical difference was found, the iodine concentration and the effective atomic number in the arterial and venous phase of metastases were higher than that of the primary lung tumor, which is consistent with the results of Deniffel et al<sup>13</sup> study, showing the degree of vascularization of metastatic tumors was higher than that of the primary tumor.

Relevant literature shows that in lung squamous cell carcinoma, the tumor cells grow rapidly in piles, the tissue structure is dense, and the microvessel density is low. Adenocarcinoma has a loose tissue structure, high microvessel density, and rich blood supply, so the degree of enhancement and the iodine content in the lesion are high.<sup>14,15</sup> Most literature, such as Bevilacqua A, etc, reported that the blood supply, enhanced

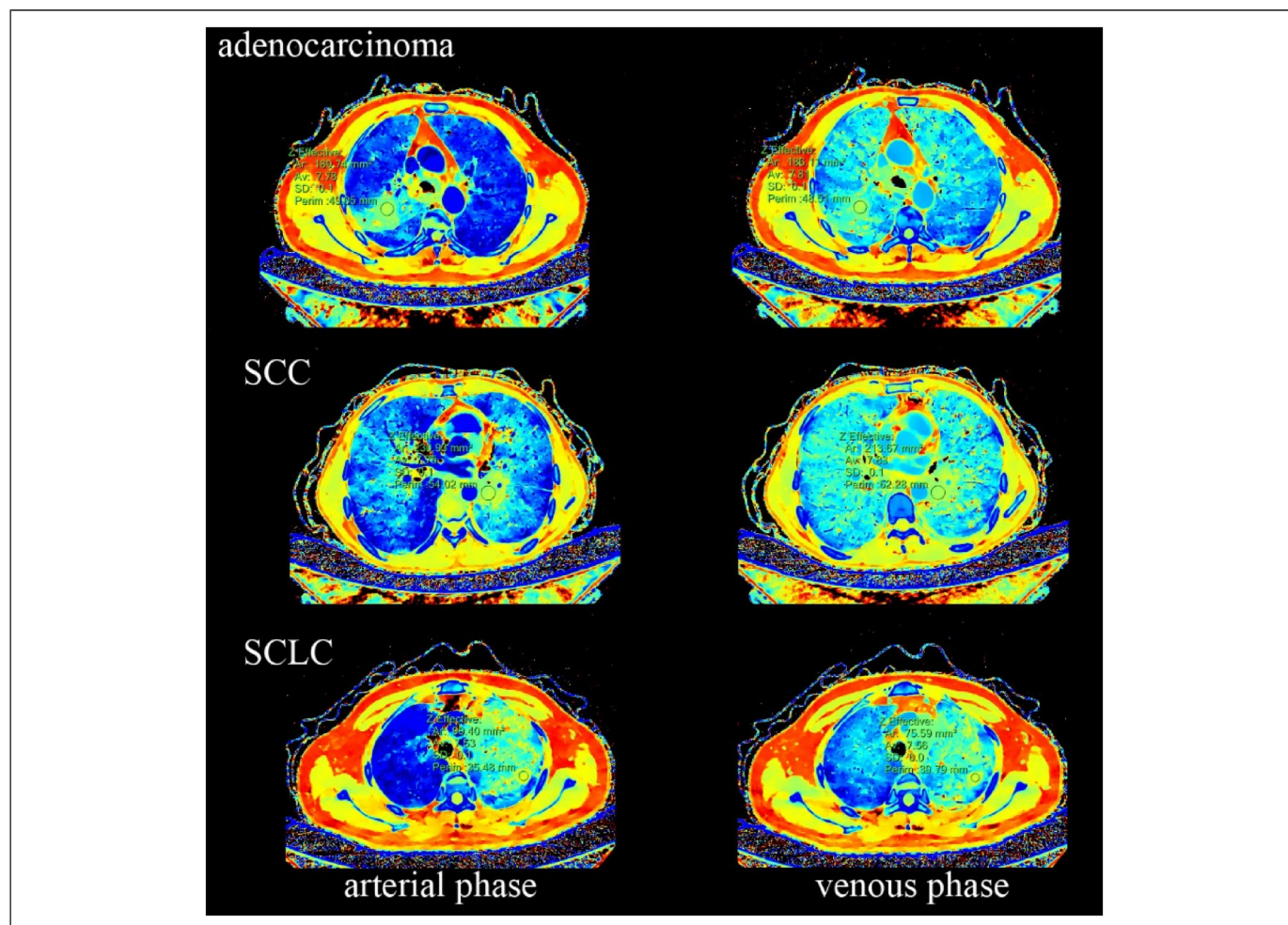


**Figure 1.** Three cases of Zeff images (arterial phase and venous phase)

scanning arteriovenous phase CT value, iodine content, and effective atomic number of adenocarcinoma was higher than squamous cell carcinoma.<sup>16</sup> However, in this study, no statistical difference was found in the arteriovenous CT value, iodine concentration, and effective atomic number between the adenocarcinoma and squamous cell carcinoma groups, which may be caused by the following reasons:

1. Squamous cell carcinoma is often accompanied by irregular necrosis within the tumor. To avoid necrosis, the surrounding area of the tumor is selected for measurement. The proliferation of blood vessels around the tumor is more active, resulting in higher enhancement values of squamous cell carcinoma. Adenocarcinoma is easily accompanied by mucus production, leading to uneven enhancement of the tumor which will result in no statistical differences in the arterial and venous phase CT value, iodine concentration, and the effective atomic number between squamous cell carcinoma and adenocarcinoma.
2. Some primary tumors of lung cancer have large tumor bodies and uneven distribution of tumor blood vessels. Therefore, measurement errors are inevitable when selecting the substantial part.
3. Since there is no absolute limit for the increase or decrease of iodine concentration, and different DECT suppliers have different accuracy of iodine measurement, the measurement of iodine density is usually relative to the difference between the lesion area of interest and the adjacent normal tissue. For example, the iodine density measurement value of small lesions with low enhancement in the high attenuation value area is extremely inaccurate and the data obtained from different image acquisition platforms cannot be compared. Research by Jacobsen et al<sup>17</sup> showed that the minimum iodine concentration that can be accurately detected by all DECT data acquisition platforms is 0.5 mg/mL. Dual-source CT can reach 0.2 mg/mL due to the best spectral separation, even if it is used the optimal thickness of the filter between 2 layers, the spectral energy separation of DLCT is still not ideal, which causes a large amount of energy overlap, and the iodine concentration value that can be accurately detected is large.<sup>17</sup>
4. Insufficient samples of squamous cell and adenocarcinoma.

While the effective atomic number depicts the material make-up of each pixel and provides a higher degree of discrimination than attenuation in HU, in the comparative analysis of adenocarcinoma, squamous cell carcinoma, and SCLC, when the HU<sub>v</sub> does not show a statistical difference, the Zeff(v) is more sensitive in discovering the difference (Figure 1 shows 3 cases of Zeff images). And the statistically significant difference discovered between metastases and SCLC in ICA also indicates an additional value of spectral indexes than conventional CT.

The findings of our study have some limitations. First, the analysis was retrospective and limited to a small sample size. Second, the number of included CT scans for similar LCAs was relatively low and, although we assessed a multitude of tumor types, no benign pulmonary lesions, and not all malignant pulmonary tumors are considered. Third, no other DECT technology was used besides DLCT as different systems are not available at our institution. Fourth, we acknowledge that additional imaging characteristics such as tumor location, size, calcifications, or presence of necrotic areas, which are an integral part of any clinical CT assessment, could have improved the credibility of our study. This study is a first step in demonstrating the difference in spectral indexes among different pathological types of lung tumors. Additionally, there are subtle differences in tissue composition that are more evident by HU quantification. So the assessment of pulmonary tumors of unknown origin should not be limited to single parameters but a combination of CT attenuation and DECT-derived parameters. Machine learning algorithms handling multiple predefined input variables or deep learning models that are capable of automatically learning and extracting imaging features are an interesting avenue for future research but will ultimately require larger data sets.<sup>13</sup>

## Conclusion

The energy spectrum parameters of DLCT have a certain clinical value in distinguishing NSCLC from SCLC in the Zeff(v) and distinguishing SCLC from a metastatic tumor in the ICA of the parenchymal part of lung tumor. It can assist in the evaluation of pathological types when pathological biopsy specimens are not available. Because this study is a single-center retrospective study and the sample size is small, and there are currently few studies using double-layer detectors to identify the pathological types of lung tumors, multicenter, and large-sample data are still needed to further confirm and explore its value.

## Acknowledgements

Not applicable.

## Author Contributions

All authors contributed to data collection, research design, and revision of research content. All authors have approved its submission.

## Authors' Note

Xia Ma and Ming Xu contributed equally to this work. This retrospective, single-center study was approved by our institutional review board, and a waiver of informed consent was obtained.

## Declaration of Conflicting Interests


The authors declared no potential conflicts of interest with respect to the research, authorship, and/or publication of this article.



## Funding

The authors received no financial support for the research and/or authorship of this article.

## ORCID iD

Xia Ma  <https://orcid.org/0000-0002-9619-2208>

## References

1. She J, Yang P, Hong Q, Bai C. Lung cancer in China: challenges and interventions. *Chest*. 2013;143(4):1117-1126.
2. Prabhakar B, Shende P, Augustine S. Current trends and emerging diagnostic techniques for lung cancer. *Biomed Pharmacother*. 2018;106:1586-1599.
3. Odisio EG, Truong MT, Duran C, de Groot PM, Godoy MC. Role of dual-energy computed tomography in thoracic oncology. *Radiol Clin North Am*. 2018;56(4):535-548.
4. Rassouli N, Etesami M, Dhanantwari A, Rajiah P. Detector-based spectral CT with a novel dual-layer technology: principles and applications. *Insights Imaging*. 2017;8(6):589-598.
5. Sánchez-Gracián CD, Pernas RO, López CT, et al. Quantitative myocardial perfusion with stress dual-energy CT: iodine concentration differences between normal and ischemic or necrotic myocardium. Initial experience. *Eur Radiol*. 2016;26(9):3199-3207.
6. Chang S, Hur J, Im DJ, et al. Dual-energy CT-based iodine quantification for differentiating pulmonary artery sarcoma from pulmonary thromboembolism: a pilot study. *Eur Radiol*. 2016;26(9):3162-3170.
7. Hokamp N G, Gilkeson R, Jordan MK, et al. Virtual monoenergetic images from spectral detector CT as a surrogate for conventional CT images: unaltered attenuation characteristics with reduced image noise. *Eur J Radiol*. 2019;117:49-55.
8. Sellerer T, Noël PB, Patino M, et al. Dual-energy CT: a phantom comparison of different platforms for abdominal imaging. *Eur Radiol*. 2018;28(7):2745-2755.
9. Spira D, Neumeister H, Spira SM, et al. Assessment of tumor vascularity in lung cancer using volume perfusion CT (VPCT) with histopathologic comparison: a further step toward an individualized tumor characterization. *J Comput Assist Tomogr*. 2013;37(1):15-21.
10. Zieliński KW, Kulig A. Morphology of the microvascular bed in primary human carcinomas of lung. Part I: three-dimensional pattern of microvascular network. *Pathol Res Pract*. 1984;178(3):243-250.
11. Zieliński KW, Kulig A, Zieliński J. Morphology of the microvascular bed in primary human carcinomas of lung. Part II. Morphometric investigations of microvascular bed of lung tumors. *Pathol Res Pract*. 1984;178(4):369-377.
12. Shi J, Schmid-Bindert G, Fink C, et al. Dynamic volume perfusion CT in patients with lung cancer: baseline perfusion characteristics of different histological subtypes. *Eur J Radiol*. 2013;82(12):e894-e900.
13. Deniffel D, Sauter A, Fingerle A, Rummeny EJ, Makowski MR, Pfeiffer D. Improved differentiation between primary lung cancer and pulmonary metastasis by combining dual-energy CT-derived biomarkers with conventional CT attenuation. *Eur Radiol*. 2021;31(2):1002-1010.
14. Tateishi U, Nishihara H, Tsukamoto E, Morikawa T, Tamaki N, Miyasaka K. Lung tumors evaluated with FDG-PET and dynamic CT: the relationship between vascular density and glucose metabolism. *J Comput Assist Tomogr*. 2002;26(2):185-190.
15. Kang MJ, Park CM, Lee CH, Goo JM, Lee HJ. Dual-energy CT: clinical applications in various pulmonary diseases. *Radiographics*. 2010;30(3):685-698.
16. Bevilacqua A, Gavelli G, Baiocco S, Barone D. CT Perfusion in patients with lung cancer: squamous cell carcinoma and adenocarcinoma show a different blood flow. *Biomed Res Int*. 2018;2018:6942131.
17. Jacobsen MC, Cressman E, Tamm EP, et al. Dual-energy CT: lower limits of iodine detection and quantification. *Radiology*. 2019;292(2):414-419.